

Direct Air-to-Underwater Optical Wireless Communication: Statistical Characterization and Outage Performance

Ziyaur Rahman, *Graduate Student Member, IEEE*, S. M. Zafaruddin, *Senior Member, IEEE*, and V. K. Chaubey, *Senior Member, IEEE*

Abstract— In general, a buoy relay is used to connect the underwater communication to the terrestrial network over a radio or optical wireless communication (OWC) link. The use of relay deployment may pose security and deployment issues. This paper investigates the feasibility of direct air-to-underwater (A2UW) communication from an over-the-sea OWC system to an underwater submarine without deploying a relaying node. We analyze the statistical performance of the direct transmission over the combined channel fading effect of atmospheric turbulence, random fog, air-to-water interface, oceanic turbulence, and pointing errors. We develop novel analytical expressions for the probability density function (PDF) and cumulative distribution function (CDF) of the resultant signal-to-noise ratio (SNR) in terms of bivariate Meijer-G and Fox-H functions. We use the derived statistical results to analyze the system performance by providing exact and asymptotic results of the outage probability in terms of system parameters. We use computer simulations to demonstrate the performance of direct A2UW transmissions compared to the relay-assisted system.

Index Terms—Atmospheric turbulence, BS distribution, fog, outage probability, underwater communications, UWOC.

I. INTRODUCTION

Optical wireless communication (OWC) is a potential technology for underwater applications such as oceanographic data collection, tactical surveillance, and offshore explorations [1]. The OWC system performs exceedingly well for underwater communication achieving ultra-high data rate secured transmission at a low-power consumption compared to legacy technologies such as acoustic waves and radio-frequency (RF). Still, the performance of underwater OWC (UWOC) is limited by the oceanic turbulence caused by air bubbles levels and variation in the temperature and pressure of the seawater in addition to other impairments such as scattering and absorption [2]–[4].

There has been an increased research interest in studying the heterogeneous underwater-terrestrial network to offload the underwater data using RF or OWC technologies. Cooperative relaying protocols such as amplify-and-forward (AF) and decode-and-forward (DF) are generally employed to interface the UWOC with terrestrial link using a buoy relay node [5]–[9]. In [7], the authors analyzed the performance of an unmanned-aerial-vehicle (UAV) assisted RF-UWOC system

using both fixed-gain AF and DF relaying protocols. The authors in [9] used the OWC transmission over Gamma-Gamma turbulence to study the fixed-gain AF relaying for the mixed UWOC-OWC communication system.

In the aforementioned and related research, the deployment of relaying devices, either floating buoys or mounted on a ship, may be challenging, and to the least, can impose security issues, especially if the underwater communication is carried out for tactical surveillance. Recently, there have been some preliminary studies for direct transmissions, specifically towards the statistical modeling of wavy water surface at the air-to-water interface [10]–[12]. The Birnbaum-Saunders distribution function was found to be a better fit to predict the statistical behavior of the fading channel in the presence of random aquatic waves at the air-to-water interface [11]. Further, Agheli *et.al* [13] presented a study for OWC transmission directly to an underwater vehicle under the impact of air-to-water interface with log-normal turbulence model for underwater communication. However, they used deterministic path loss and did not consider atmospheric turbulence for the OWC link, which may overestimate the actual performance. It should be mentioned that foggy weather conditions over the sea may randomly change the optical signal absorption, precluding deterministic path loss for the OWC link [14], [15]. Moreover, the log-normal model for the underwater is limited for weak oceanic turbulence. To the best of the author's knowledge, generalized fading models for atmospheric and oceanic turbulence have not yet been studied for the direct UWOC system. It requires novel approaches for statistically analyzing the system performance considering the different channel coefficients involved in the signal transmission.

In this paper, we investigate the feasibility of direct air-to-underwater (A2UW) communication from an over-the-sea OWC system to an underwater submarine under generalized channel conditions. We analyze the statistical performance of the proposed scheme by considering the combined channel effect of atmospheric turbulence, random fog, air-to-water interface, oceanic turbulence, and pointing errors. We consider the generalized Malága distribution for the atmospheric turbulence, Gamma distributed attenuation coefficient for random fog, the BS distribution to model the aquatic waves at air-water interface, the mixture exponential-generalized gamma (EGG) distribution for the oceanic turbulence, and zero-boresight for random misalignment errors between transmitter and detector. We develop novel analytical expressions for the probability density function (PDF) and cumulative distribution function (CDF) of the resultant signal-to-noise ratio (SNR) for the A2UW using the bivariate Fox's H-function. We use the

This work was supported in part by the Science and Engineering Research Board (SERB), India under MATRICS Grant MTR/2021/000890 and Start-up Research Grant SRG/2019/002345.

The authors are with the Department of Electrical and Electronics Engineering, Birla Institute of Technology and Science, Pilani, Pilani-333031, Rajasthan, India. (Email: {p20170416, syed.zafaruddin, vkc}@pilani.bits-pilani.ac.in.

derived statistical results to analyze the system performance by providing exact outage probability in terms of system parameters. We also analyze the outage performance asymptotically to derive diversity order providing insights on the system behavior in the high SNR regime. We validate our derived analysis and use computer simulations to demonstrate the performance of the direct A2UW scheme with a comparison to the DF-based relay-assisted system. The direct A2UW can provide acceptable performance for various scenarios of interest when the double fading effect above-the-sea and underwater channels is not severe.

II. SYSTEM AND CHANNEL MODELS

We consider an A2UW transmission scheme where an over-the-sea UAV directly communicates with an underwater submarine. The UAV transmits a source signal using the intensity modulation/direct-detection (IM/DD) technique for the destination located in underwater. The transmitted signal encounters fading due to atmospheric turbulence, random fog, oceanic turbulence, and pointing errors. In addition to these channel fading impairments, the signal is affected by erratic random and non-random aquatic waves at the air-water interface. We consider link without breaking waves (i.e., no bubbles) at the air-water interface. Thus, the electrical signal received (denoted by y) at the underwater detector can be expressed as

$$y = h_{at}h_f h_{ws} H_w h_{ut} h_p s + n \quad (1)$$

where s is the transmitted signal, h_{at} is the channel coefficient for the atmospheric turbulence, h_f models the randomness in the path gain due to the foggy condition, h_{ws} models the effect of scattering and reflection of the signal by water waves at the air-to-water interface, H_w denotes the oceanic path gain, h_{ut} is the oceanic turbulence, h_p is the channel coefficient due to the pointing errors, and n denotes the additive noise at the detector with variance σ_n^2 . The parameterized values of the channel coefficients in (1) are given in Table I.

We consider the generalized Malága distribution $f_{h_{at}}(x) = A_{mg} \sum_{m=1}^{\beta} \alpha_m x K_{\alpha_M - m} (2\sqrt{\frac{\alpha_M \beta M x}{g \beta M + \Omega'}})$ to model the atmospheric turbulence, where the fading parameters α_M , β_M , A_{mg} , a_m , g , and Ω' are defined in [16]. The probability density function (PDF) of the foggy channel is given as [14]:

$$f_{h_f}(x) = \frac{z^k}{\Gamma(k)} \left(\log \frac{1}{x} \right)^{k-1} x^{z-1}, \quad 0 < x \leq 1 \quad (2)$$

where $z = 4.343/\beta_f d_{air}$, $k > 0$ is the shape parameter, $\beta_f > 0$ is the scale parameter and d_{air} (in km) is link distance from the water surface to the UAV. For the deterministic path gain, we can use the visibility model $h_f = e^{-\phi_{air} d_{air}}$, where ϕ_{air} is the attenuation coefficient [17]. The statistical characterization of the air-to-water interface is captured through Birnbaum-Saunders (BS) distribution [11]:

$$f_{h_{ws}}(x) = \frac{1}{2\sqrt{2\pi\alpha\beta}} \left[\left(\frac{\beta}{x} \right)^{1/2} + \left(\frac{\beta}{x} \right)^{3/2} \right] \exp \left[-\frac{1}{2\alpha^2} \left(\frac{x}{\beta} + \frac{\beta}{x} - 2 \right) \right] \quad (3)$$

where $\alpha > 0$ and $\beta > 0$ are the shape and scale parameters to parameterize the BS distribution. The path gain for the oceanic turbulence can be approximated using Beer-Lambert law $H_w = e^{-\phi_{water} d_{water}}$ (d_{water} in m) [13], where ϕ_{water}

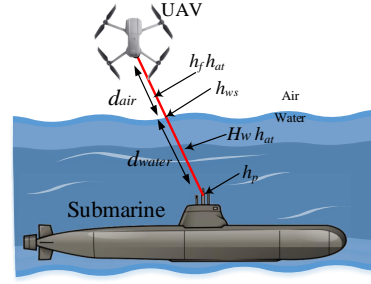


Fig. 1. A schematic diagram for direct A2UW communication.

is the extinction attenuation coefficient. Further, we use the recently proposed mixture EGG distribution for the oceanic turbulence (caused by air bubbles and temperature gradient) [4]:

$$f_{h_{ut}}(x) = \frac{\omega}{\lambda} \exp\left(-\frac{x}{\lambda}\right) + (1 - \omega) \frac{cx^{ac-1} \exp\left(-\left(\frac{x}{b}\right)^c\right)}{b^{ac} \Gamma(a)} \quad (4)$$

where ω is the mixture coefficient of the distributions (i.e, $0 < \omega < 1$), λ is the exponential distribution parameter, a , b , and c are the generalized Gamma distribution parameters. Finally, we model the misalignment between the transmit aperture of UAV and detector at the submarine using the PDF $f_{h_p}(x) = \frac{\rho^2}{A_0^2} x^{\rho^2-1}$, where A_0 and ρ are pointing error parameters [18].

III. STATISTICAL CHARACTERIZATION

In this section, we statistically characterize the direct transmission by deriving PDF and CDF of the SNR for the combined channel effect consisting of over-the-sea and underwater fading channels.

We define $\gamma = \gamma_0 |h|^2$ as the SNR for the system model of (1), where the combined channel $h = h_{at} h_f h_{ws} h_{ut} h_p$ with $\gamma_0 = 2P_s^2 R^2 H_w^2 / \sigma_n^2$, P_s is the average optical transmitted power, and R is the responsivity. In the following theorem, we develop PDF of the SNR for the direct transmission scheme as given in (1), considering fading models of atmospheric turbulence, random fog, air-to-water interface, oceanic turbulence, and pointing errors. It should be mentioned that direct application of the product of random variables is not readily applicable to derive the PDF of SNR for the A2UW.

Theorem 1: If $\{\alpha_M, \beta_M, A_{mg}, a_m, g, \Omega'\}$ models the atmospheric turbulence, $\{z = 4.343/\beta_f d, k\}$ models the random fog, $\{\alpha, \beta\}$ models the air-to-water interface, $\{\omega, \lambda, a, b, c\}$ models the oceanic turbulence, and $\{\rho, A_0\}$ models the pointing errors, then the PDF of SNR γ for the direct A2UW scheme is given in (5) (see top of the next page).

Proof: The proof is presented in Appendix A. ■

It should be mentioned that standard functions are available in MATLAB and MATHEMATICA to compute bivariate Meijer-G and Fox-H functions.

IV. OUTAGE PROBABILITY

We use the derived statistical results to study the outage probability of the system as a performance metric to compare with the relay-assisted transmissions. Note that other statistical performance metrics such as average BER and ergodic capacity can be similarly derived.

A. Exact Analysis

We can use (5) to develop an exact outage probability of the considered system for a given threshold SNR γ_{th} as $P_{out} =$

$$\begin{aligned}
f_\gamma(\gamma) &= \frac{z^k \rho^2 A_{\text{mg}} \omega}{8\sqrt{\pi} \gamma} \exp\left(\frac{1}{\alpha^2}\right) \sum_{m=1}^{\beta_m} b_m G_{1,0:1,0:4+k,1+k}^{0,1:0,1:0,4+k} \left(\frac{1}{2} \mid - \mid \zeta_1 \mid 4\alpha^4, \frac{2\alpha^2 \beta (g\beta_m + \Omega') A_0 \lambda}{\alpha_m \beta_m} \sqrt{\frac{\gamma_0}{\gamma}} \right) \\
&+ \frac{z^k \rho^2 A_{\text{mg}} \omega}{16\sqrt{\pi} \alpha^2 \gamma} \exp\left(\frac{1}{\alpha^2}\right) \sum_{m=1}^{\beta_m} b_m G_{1,0:1,0:4+k,1+k}^{0,1:0,1:0,4+k} \left(\frac{3}{2} \mid - \mid \zeta_1 \mid 4\alpha^4, \frac{2\alpha^2 \beta (g\beta_m + \Omega') A_0 \lambda}{\alpha_m \beta_m} \sqrt{\frac{\gamma_0}{\gamma}} \right) \\
&+ \frac{z^k \rho^2 A_{\text{mg}}}{8\sqrt{\pi} \gamma} \frac{1-\omega}{\Gamma(a)} \exp\left(\frac{1}{\alpha^2}\right) \sum_{m=1}^{\beta_m} b_m H_{1,0:1,0:4+k,1+k}^{0,1:0,1:0,4+k} \left(\frac{\zeta_2}{\chi_2} \mid 4\alpha^4, \frac{2\alpha^2 \beta (g\beta_m + \Omega') A_0 b}{\alpha_m \beta_m} \sqrt{\frac{\gamma_0}{\gamma}} \right) \\
&+ \frac{z^k \rho^2 A_{\text{mg}}}{16\sqrt{\pi} \alpha^2 \gamma} \frac{1-\omega}{\Gamma(a)} \exp\left(\frac{1}{\alpha^2}\right) \sum_{m=1}^{\beta_m} b_m H_{1,0:1,0:4+k,1+k}^{0,1:0,1:0,4+k} \left(\frac{\zeta_3}{\chi_2} \mid 4\alpha^4, \frac{2\alpha^2 \beta (g\beta_m + \Omega') A_0 b}{\alpha_m \beta_m} \sqrt{\frac{\gamma_0}{\gamma}} \right) \quad (5)
\end{aligned}$$

where $\zeta_1 = \{0, 1 - \rho^2, 1 - \alpha_m, 1 - m, \{1 - z\}_1^k\}$, $\chi_1 = \{-\rho^2, \{-z\}_1^k\}$, $\zeta_2 = \{(\frac{1}{2}; 1, 1) : (1, 1); (1 - a, \frac{1}{c}), (1 - \rho^2, 1), (1 - \alpha_m, 1), (1 - m, 1), (\{1 - z\}_1^k, 1)\}$, $\chi_2 = \{- : -; (-\rho^2, 1), (\{-z\}_1^k, 1)\}$, and $\zeta_3 = \{(\frac{3}{2}; 1, 1) : (1, 1); (1 - a, \frac{1}{c}), (1 - \rho^2, 1), (1 - \alpha_m, 1), (1 - m, 1), (\{1 - z\}_1^k, 1)\}$.

$$\begin{aligned}
P_{\text{out}} &= \frac{z^k \rho^2 A_{\text{mg}} \omega}{4\sqrt{\pi}} \exp\left(\frac{1}{\alpha^2}\right) \sum_{m=1}^{\beta_m} b_m G_{1,0:1,0:5+k,2+k}^{0,1:0,1:1,4+k} \left(\frac{1}{2} \mid - \mid \zeta_4 \mid 4\alpha^4, \frac{2\alpha^2 \beta (g\beta_m + \Omega') A_0 \lambda}{\alpha_m \beta_m} \sqrt{\frac{\gamma_0}{\gamma_{\text{th}}}} \right) \\
&+ \frac{z^k \rho^2 A_{\text{mg}} \omega}{8\sqrt{\pi} \alpha^2} \exp\left(\frac{1}{\alpha^2}\right) \sum_{m=1}^{\beta_m} b_m G_{1,0:1,0:5+k,2+k}^{0,1:0,1:1,4+k} \left(\frac{3}{2} \mid - \mid \zeta_4 \mid 4\alpha^4, \frac{2\alpha^2 \beta (g\beta_m + \Omega') A_0 \lambda}{\alpha_m \beta_m} \sqrt{\frac{\gamma_0}{\gamma_{\text{th}}}} \right) \\
&+ \frac{z^k \rho^2 A_{\text{mg}}}{4\sqrt{\pi}} \frac{1-\omega}{\Gamma(a)} \exp\left(\frac{1}{\alpha^2}\right) \sum_{m=1}^{\beta_m} b_m H_{1,0:1,0:5+k,2+k}^{0,1:0,1:1,4+k} \left(\frac{\zeta_5}{\chi_5} \mid 4\alpha^4, \frac{2\alpha^2 \beta (g\beta_m + \Omega') A_0 b}{\alpha_m \beta_m} \sqrt{\frac{\gamma_0}{\gamma_{\text{th}}}} \right) \\
&+ \frac{z^k \rho^2 A_{\text{mg}}}{8\sqrt{\pi} \alpha^2} \frac{1-\omega}{\Gamma(a)} \exp\left(\frac{1}{\alpha^2}\right) \sum_{m=1}^{\beta_m} b_m H_{1,0:1,0:5+k,2+k}^{0,1:0,1:1,4+k} \left(\frac{\zeta_6}{\chi_5} \mid 4\alpha^4, \frac{2\alpha^2 \beta (g\beta_m + \Omega') A_0 b}{\alpha_m \beta_m} \sqrt{\frac{\gamma_0}{\gamma_{\text{th}}}} \right) \quad (6)
\end{aligned}$$

where $\zeta_4 = \{0, 1 - \rho^2, 1 - \alpha_m, 1 - m, \{1 - z\}_1^k, 1\}$, $\chi_4 = \{0, -\rho^2, \{-z\}_1^k\}$, $\zeta_5 = \{(\frac{1}{2}; 1, 1) : (1, 1); (1 - a, \frac{1}{c}), (1 - \rho^2, 1), (1 - \alpha_m, 1), (1 - m, 1), (\{1 - z\}_1^k, 1), (1, 1)\}$, $\chi_5 = \{- : (0, 1); (-\rho^2, 1), (\{-z\}_1^k, 1)\}$, and $\zeta_6 = \{(\frac{3}{2}; 1, 1) : (1, 1); (1 - a, \frac{1}{c}), (1 - \rho^2, 1), (1 - \alpha_m, 1), (1 - m, 1), (\{1 - z\}_1^k, 1), (1, 1)\}$.

$$\begin{aligned}
P_{\text{out}}^\infty &= \frac{z^k \rho^2 A_{\text{mg}} \omega}{4\sqrt{\pi}} \exp\left(\frac{1}{\alpha^2}\right) \sum_{m=1}^{\beta_m} b_m \sum_{i=1}^{4+k} \Gamma\left(\frac{3}{2} + \mathcal{A}_i\right) \frac{\prod_{j=1, j \neq i}^{4+k} \Gamma(\mathcal{A}_i - \mathcal{A}_j) \Gamma(1 - \mathcal{A}_i)}{\prod_{j=1}^{2+k} \Gamma(\mathcal{A}_i + \mathcal{B}_j) \Gamma(2 - \mathcal{A}_j)} \left(\frac{2\alpha^2 \beta (g\beta_m + \Omega') A_0 \lambda}{\alpha_m \beta_m} \sqrt{\frac{\gamma_0}{\gamma}} \right)^{\mathcal{A}_i - 1} \\
&+ \frac{z^k \rho^2 A_{\text{mg}} \omega}{8\sqrt{\pi} \alpha^2} \exp\left(\frac{1}{\alpha^2}\right) \sum_{m=1}^{\beta_m} b_m \sum_{i=1}^{4+k} \Gamma\left(\frac{1}{2} + \mathcal{A}_i\right) \frac{\prod_{j=1, j \neq i}^{4+k} \Gamma(\mathcal{A}_i - \mathcal{A}_j) \Gamma(1 - \mathcal{A}_i)}{\prod_{j=1}^{2+k} \Gamma(\mathcal{A}_i + \mathcal{B}_j) \Gamma(2 - \mathcal{A}_j)} \left(\frac{2\alpha^2 \beta (g\beta_m + \Omega') A_0 \lambda}{\alpha_m \beta_m} \sqrt{\frac{\gamma_0}{\gamma}} \right)^{\mathcal{A}_i - 1} \\
&+ \frac{z^k \rho^2 A_{\text{mg}}}{4\sqrt{\pi}} \frac{1-\omega}{\Gamma(a)} \exp\left(\frac{1}{\alpha^2}\right) \sum_{m=1}^{\beta_m} b_m \sum_{i=1}^{4+k} \sum_{i=1}^{4+k} \frac{1}{\mathcal{Q}_i} \Gamma\left(\frac{3}{2} + \mathcal{P}_i\right) \frac{\Gamma(-(\mathcal{P}_i - 1) \frac{\mathcal{T}_i}{\mathcal{Q}_i}) \prod_{j=1, j \neq i}^{4+k} \Gamma(1 + \mathcal{P}_j + (\mathcal{P}_i - 1) \frac{\mathcal{Q}_j}{\mathcal{Q}_i})}{\Gamma(1 - (\mathcal{P}_i - 1) \frac{1}{\mathcal{Q}_i}) \prod_{j=1}^{2+k} \Gamma(1 - \mathcal{S}_j + (\mathcal{P}_i - 1) \frac{\mathcal{T}_j}{\mathcal{Q}_i})} \\
&\quad \left(\frac{2\alpha^2 \beta (g\beta_m + \Omega') A_0 b}{\alpha_m \beta_m} \sqrt{\frac{\gamma_0}{\gamma}} \right)^{(\mathcal{P}_i - 1) / \mathcal{Q}_i} + \frac{z^k \rho^2 A_{\text{mg}}}{8\sqrt{\pi} \alpha^2} \frac{1-\omega}{\Gamma(a)} \exp\left(\frac{1}{\alpha^2}\right) \sum_{m=1}^{\beta_m} \sum_{i=1}^{4+k} \sum_{i=1}^{4+k} \frac{1}{\mathcal{Q}_i} \\
&\quad \Gamma\left(\frac{1}{2} + a_i\right) \frac{\Gamma(-(a_i - 1) \frac{\beta_j}{\mathcal{P}_i}) \prod_{j=1, j \neq i}^{4+k} \Gamma(1 + \mathcal{P}_j + (\mathcal{P}_i - 1) \frac{\mathcal{Q}_j}{\mathcal{Q}_i})}{\Gamma(1 - (\mathcal{P}_i - 1) \frac{1}{\mathcal{Q}_i}) \prod_{j=1}^{2+k} \Gamma(1 - \mathcal{S}_j + (\mathcal{P}_i - 1) \frac{\mathcal{T}_j}{\mathcal{Q}_i})} \left(\frac{2\alpha^2 \beta (g\beta_m + \Omega') A_0 b}{\alpha_m \beta_m} \sqrt{\frac{\gamma_0}{\gamma}} \right)^{(\mathcal{P}_i - 1) / \mathcal{Q}_i} \quad (7)
\end{aligned}$$

where $\mathcal{A}_i = \mathcal{A}_j = \{0, 1 - \rho^2, 1 - \alpha_m, 1 - m, \{1 - z\}_1^k, 1\}$, $\mathcal{B}_i = \mathcal{B}_j = \{0, -\rho^2, \{-z\}_1^k\}$, $\mathcal{P}_i = \mathcal{P}_j = \{1 - a, 1 - \rho^2, 1 - \alpha_m, 1 - m, \{1 - z\}_1^k, 1\}$, and $\mathcal{Q}_i = \mathcal{Q}_j = \{\frac{1}{c}, 1, 1, 1, \{1\}_1^k, 1\}$, $\mathcal{S}_i = \mathcal{S}_j = \{-\rho^2, \{-z\}_1^k\}$, $\mathcal{T}_i = \mathcal{T}_j = \{1, \{1\}_1^k\}$.

$P[\gamma < \gamma_{\text{th}}]$. Thus, we substitute (5) in $P_{\text{out}} = \int_0^{\gamma_{\text{th}}} f_\gamma(\gamma) d\gamma$ and apply standard Mathematical as used in deriving the PDF to get the outage probability in (6).

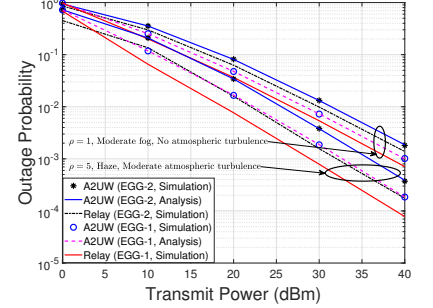
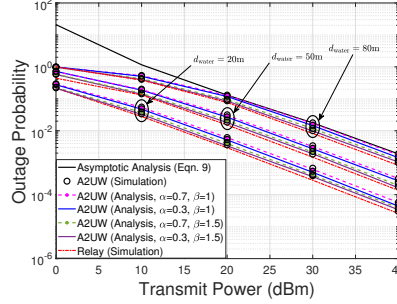
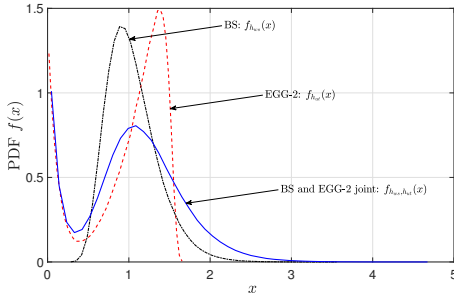
B. Asymptotic Analysis

Although (6) can provide outage probability over a wide range of γ_0 , it is desirable to analyze the outage probability asymptotically at a high SNR $\gamma_0 \rightarrow \infty$. Thus, we use the asymptotic result of a single-variate Fox-H function in [19, Th. 1.11] and multivariate Fox-H [20] to express the outage probability in the high SNR regime as presented in (7).

C. Diversity Order

Compiling the dominant terms of γ_0 in (7) and using the definitions \mathcal{A}_i , \mathcal{P}_i , and \mathcal{Q}_i , the diversity order for the A2UW

can be expressed as $G_{\text{out}} = \min\{\frac{1}{2}, \frac{\alpha_m}{2}, \frac{\beta_m}{2}, \frac{z}{2}, \frac{ac}{2}, \frac{\rho^2}{2}\}$. It can be seen that the diversity order in [4] [9] becomes a special case of our generalized model, which includes random fog and air-to-water interface in addition to the atmospheric and oceanic turbulence with pointing errors. The diversity order reveals several interesting behaviors of the outage probability for the direct A2UW transmission, specifically: (i) it is independent of the fading parameters of the BS distribution modeled for the air-to-water interface; and (ii) the diversity order is $\frac{1}{2}$ or $\frac{z}{2}$ if $z (= \frac{4.343}{\beta_f d_{\text{air}}}) < 1$ depending on the density fog and d_{air} since measurement data reveals that typically $ac > 1$, $\alpha_M > 1$, $\beta_M > 1$, and $\rho > 1$ can be maintained with higher beam-width to reduce the impact of pointing errors.



(a) PDF of combined air-to-water interface and oceanic turbulence.. (b) EGG-2, light fog, weak atmospheric turbulence, (c) $\alpha = 0.3$, $\beta = 1$; $d_{\text{air}} = 20\text{m}$, $d_{\text{water}} = 50\text{m}$. $\rho = 5$, $A_0 = 0.0032$.

Fig. 2. Direct A2UW transmission with a comparison to the relay-assisted system.

TABLE I
SIMULATION PARAMETERS

Noise	$\sigma_n^2 = 10^{-14} \text{ A}^2/\text{GHz}$
Light Fog	$k = 2.32$, $\beta_f = 13.12$
Moderate Fog	$k = 5.49$, $\beta_f = 12.06$
Atten. Coeff. (Haze)	$\phi_{\text{air}} = 0.98$ [17]
Atten. Coeff. (UW)	$\phi_{\text{water}} = 21.79 \text{ dB/km}$ [13]
EGG-1 (Weaker)	$\omega = 0.21$, $\lambda = 0.329$ $a = 1.429$, $b = 1.181$, $c = 17.198$
EGG-2 (Strong)	$\omega = 0.458$, $\lambda = 0.344$ $a = 1.042$, $b = 1.576$, $c = 35.942$
BS Distribution	$\alpha = \{0.3, 0.7\}$, $\beta = \{1, 1.5\}$

V. SIMULATION RESULTS AND DISCUSSIONS

We use MATLAB software to validate our analysis and demonstrate the performance of the direct A2UW transmission considering various system and channel configurations. We also compare the performance with the DF-based relaying to better assess use cases for the proposed scheme. We fix the air-to-water surface link distance d_{air} from 20m (for example, a UAV hovering over the sea), and consider underwater link range d_{water} from 20m to 80m. We use three atmospheric turbulence (weak, medium, and strong) [16] and consider low $\rho = 5$ and high $\rho = 1$ pointing errors with $A_0 = 0.0032$. Other simulation parameters are listed in Table I.

First, we demonstrate the effect of fading due to the aquatic waves at the air-to-water interface by comparing PDF of the combined BS and EGG distributions with the EGG, as shown in Fig. 2(a). The figure depicts that the BS distribution deteriorates random channel conditions for the direct A2UW transmission since the probability of getting the peak value decreases as compared with the EGG. However, the PDF plot of $f_{h_{ws}h_{ut}}(x)$ reveals that the average value of the combined channel may increase due to higher non-zero values compared with the EGG alone.

Next, we compare the outage probability of the direct A2UW transmission with the DF relay system at three different underwater distances $d_{\text{water}} = 20\text{m}$, $d_{\text{water}} = 50\text{m}$,

and $d_{\text{water}} = 80\text{m}$, as shown in Fig. 2(b). The atmospheric turbulence is considered to be weak, which is a reasonable assumption at such a short distance. The figure shows that the direct A2UW transmission achieves performance close to the relay-assisted system for different underwater link distances. However, there is a gap in the performance 2dBm when the BS parameters become $\alpha = 0.7$ and $\beta = 1$. Fig. (2) also demonstrates that the effect of BS parameters (α , β) on the outage probability is marginal, and the slope remains constant, which confirms our analysis for the diversity order.

Finally, in Fig. 2(c), we demonstrate the interplay of oceanic turbulence, pointing errors, atmospheric turbulence, and fog density on the outage performance. The figure shows that the A2UW performs close to the relayed system for both strong and weaker oceanic turbulence scenarios without atmospheric turbulence. However, the direct transmission incurs a penalty of 4dBm transmit power to achieve the exact outage probability of the relayed system in the presence of atmospheric turbulence. The degradation in the A2UW performance occurs due to the double fading effect of turbulence and path gain of two mediums for the direct A2UW transmissions compared with the dominant single link performance using the DF protocol. The figure also confirms the relative effect of pointing errors ($\rho = 1$ and $\rho = 5$) and intensity of oceanic turbulence (EGG-1 and EGG-2) on wireless transmissions.

We can conclude that the direct A2UW achieves acceptable performance for various scenarios of interest and performs close to the relay-assisted transmissions when the double fading effect caused by the cascading of above-the-sea and underwater channels is not severe. Nevertheless, relay-assisted transmission is optimal in the mixed OWC-UWOC transmission. Experimental demonstration are further required to support the theoretical analysis developed in this paper. We envision that the proposed direct A2UW transmission may further substantiate underwater communications using optical carriers.

APPENDIX A: PDF OF SNR

To derive the PDF of the product of 5 random variables, we express $h = h_1 h_f h_{ws} h_{ut}$, where $h_1 = h_{at} h_p$. The PDF of h_1 is given in [21]

$$f_{h_1}(x) = \frac{\rho^2 A_{\text{mg}}}{2x} \sum_{m=1}^{\beta_M} b_m G_{1,3}^{3,0} \left(\frac{\alpha_M \beta_M}{g \beta_M + \Omega'} \frac{x}{A_0} \middle| \begin{matrix} \rho^2 + 1 \\ \rho^2, \alpha_M, m \end{matrix} \right) \quad (8)$$

Next, we express $h = h_2 h_{ws} h_{ut}$, where $h_2 = h_1 h_f$. Substituting (2) and (8) in $f_{h_2}(x) = \int_x^\infty \frac{1}{|h_1|} f_{h_f}(h_2|h_1) f_{h_1}(h_1) dh_1$, we get

$$f_{h_2}(x) = \frac{\rho^2 A_{mg}}{2h_1} x^{z-1} \int_x^\infty h_1^{-z-1} \left[\ln\left(\frac{h_1}{x}\right) \right]^{k-1} \sum_{m=1}^{\beta_M} b_m G_{1,3}^{3,0} \left(\frac{\alpha_M \beta_M}{g \beta_M + \Omega'} \frac{h_1}{A_0} \left| \begin{matrix} \rho^2 + 1 \\ \rho^2, \alpha_M, m \end{matrix} \right. \right) dh_1 \quad (9)$$

Using the definition of Meijer-G function and substituting $\ln(h_1/x) = t$, we solve the inner integral $\int_0^\infty t^{k-1} \exp(-(z-s)t) dt = \frac{\Gamma(k)}{(z-s)^k} = \Gamma(k) \left[\frac{\Gamma(z-s)}{\Gamma(1+z-s)} \right]^k$ in terms of the Gamma function, and apply the definition of the Meijer-G function to get the PDF of h_2 :

$$f_{h_2}(x) = \frac{z^k \rho^2 A_{mg}}{2x} \sum_{m=1}^{\beta_M} b_m G_{1+k,3+k}^{3+k,0} \left(\rho^2 + 1, \{z+1\}_1^k \left| \begin{matrix} \alpha_m \beta_m x \\ (g \beta_m + \Omega') A_0 \end{matrix} \right. \right) \quad (10)$$

Note that the PDF in (10) can be verified using the unified expression in [22].

Next, we express $h = h_3 h_{ut}$, where $h_3 = h_2 h_{ws}$. The product distribution of h_3 can be expressed as

$$f_{h_3}(x) = \int_0^\infty \frac{1}{|h_{ws}|} f_{h_2}(h_3/h_{ws}) f_{h_{ws}}(h_{ws}) dh_{ws} \quad (11)$$

Since the direct use of (3) in (11) becomes intractable, we convert the PDF of BS distribution in (3) as

$$f_{h_{ws}}(h_{ws}) = \frac{1}{2\sqrt{2\pi\alpha\beta}} \exp\left(\frac{1}{\alpha^2}\right) \left(\frac{\beta}{h_{ws}}\right)^{1/2} G_{0,1}^{1,0} \left(- \left| \frac{h_{ws}}{2\alpha^2\beta} \right. \right) G_{0,1}^{1,0} \left(- \left| \frac{\beta}{2\alpha^2 h_{ws}} \right. \right) + \frac{1}{2\sqrt{2\pi\alpha\beta}} \exp\left(\frac{1}{\alpha^2}\right) \left(\frac{\beta}{h_{ws}}\right)^{3/2} G_{0,1}^{1,0} \left(- \left| \frac{h_{ws}}{2\alpha^2\beta} \right. \right) G_{0,1}^{1,0} \left(- \left| \frac{\beta}{2\alpha^2 h_{ws}} \right. \right) \quad (12)$$

Substituting (10) and (12) in (11) with the identity $G_{p,q}^{m,n} \left(\begin{matrix} a_p \\ b_q \end{matrix} \middle| z \right) = G_{q,p}^{n,m} \left(\begin{matrix} 1-b_q \\ 1-a_p \end{matrix} \middle| z^{-1} \right)$ and applying the identity [23, eq. 07.34.21.0081.01], we get

$$f_{h_3}(x) = \frac{z^k \rho^2 A_{mg}}{4\sqrt{\pi}x} \exp\left(\frac{1}{\alpha^2}\right) \sum_{m=1}^{\beta_M} b_m G_{1,0:1,0:3+k}^{0,1:0,1:0,3+k} \left(\begin{matrix} \frac{1}{2} \\ - \end{matrix} \middle| \begin{matrix} 1 \\ - \end{matrix} \middle| \begin{matrix} \zeta_7 \\ \chi_7 \end{matrix} \middle| 4\alpha^4, \frac{2\alpha^2\beta(g\beta_m + \Omega')A_0}{\alpha_m \beta_m x} \right) + \frac{z^k \rho^2 A_{mg}}{8\sqrt{\pi}\alpha^2 x} \exp\left(\frac{1}{\alpha^2}\right) \sum_{m=1}^{\beta_M} b_m G_{1,0:1,0:3+k}^{0,1:0,1:0,3+k} \left(\begin{matrix} \frac{3}{2} \\ - \end{matrix} \middle| \begin{matrix} 1 \\ - \end{matrix} \middle| \begin{matrix} \zeta_7 \\ \chi_7 \end{matrix} \middle| 4\alpha^4, \frac{2\alpha^2\beta(g\beta_m + \Omega')A_0}{\alpha_m \beta_m x} \right) \quad (13)$$

where $\zeta_7 = \{1 - \rho^2, 1 - \alpha_m, 1 - m, \{1 - z\}_1^k\}$, $\chi_7 = -\rho^2, \{-z\}_1^k$. Finally, we use (4) and (13) in $f_h(x) = \int_0^\infty \frac{1}{|h_{ut}|} f_{h_3}(h/h_{ut}) f_{h_{ut}}(h_{ut}) dh_{ut}$, and apply the line integral definition of Meijer-G and fox-H functions to get the PDF of $h = h_3 h_{ut}$ by solving four inner integrals as $I_1 = I_2 = \int_0^\infty h_{ut}^{s_2} \exp\left(-\frac{h_{ut}}{\lambda}\right) dh_{ut} = \lambda^{1+s_2} \Gamma(1+s_2)$, and $I_3 = I_4 = \int_0^\infty h_{ut}^{ac+s_2-1} \exp\left(-\left(\frac{h_{ut}}{\lambda}\right)^c\right) dh_{ut} = \frac{\Gamma(a+\frac{s_2}{c})}{c\lambda^{ac+s_2}}$, and apply the definitions of bivariate Meijer-G and Fox-H functions [24] with the transformation $h = \sqrt{\frac{\gamma}{\gamma_0}}$ to get the PDF of SNR γ in (5).

REFERENCES

- [1] Z. Zeng *et al.*, "A survey of underwater optical wireless communications," *IEEE Commun. Surveys Tuts.*, vol. 19, no. 1, pp. 204–238, 2017.
- [2] H. M. Oubei *et al.*, "Simple statistical channel model for weak temperature-induced turbulence in underwater wireless optical communication systems," *Opt. Lett.*, vol. 42, no. 13, pp. 2455–2458, Jul 2017.
- [3] M. V. Jamali *et al.*, "Statistical studies of fading in underwater wireless optical channels in the presence of air bubble, temperature, and salinity random variations," *IEEE Trans. Commun.*, vol. 66, no. 10, pp. 4706–4723, 2018.
- [4] E. Zedini *et al.*, "Unified statistical channel model for turbulence-induced fading in underwater wireless optical communication systems," *IEEE Trans. Commun.*, vol. 67, no. 4, pp. 2893–2907, 2019.
- [5] H. Lei *et al.*, "Performance analysis of Dual-Hop RF-UWOC systems," *IEEE Photon. J.*, vol. 12, no. 2, pp. 1–15, 2020.
- [6] S. Li *et al.*, "Performance analysis of mixed RF-UWOC dual-hop transmission systems," *IEEE Trans. Veh. Technol.*, vol. 69, no. 11, pp. 14 043–14 048, 2020.
- [7] —, "Performance analysis of UAV-based mixed RF-UWOC transmission systems," *IEEE Trans. Commun.*, vol. 69, no. 8, pp. 5559–5572, 2021.
- [8] I. S. Ansari *et al.*, "Outage and error analysis of dual-hop TAS/MRC MIMO RF-UWOC systems," *IEEE Trans. Veh. Technol.*, vol. 70, no. 10, pp. 10 093–10 104, 2021.
- [9] L. Yang *et al.*, "On the performance of mixed FSO-UWOC dual-hop transmission systems," *IEEE Wireless Commun. Lett.*, vol. 10, no. 9, pp. 2041–2045, 2021.
- [10] P. Nabavi *et al.*, "Performance analysis of air-to-water optical wireless communication using SPADs," in *2019 IEEE Glob. Commun. Conf. (GLOBECOM)*, 2019, pp. 1–6.
- [11] —, "Empirical modeling and analysis of water-to-air optical wireless communication channels," in *2019 IEEE Int. Conf. Commun. Workshops (ICC Workshops)*, 2019, pp. 1–6.
- [12] T. Lin *et al.*, "Preliminary characterization of coverage for water-to-air visible light communication through wavy water surface," *IEEE Photon. J.*, vol. 13, no. 1, pp. 1–13, 2021.
- [13] P. Agheli *et al.*, "UAV-assisted underwater sensor networks using RF and optical wireless links," *J. Lightw. Technol.*, vol. 39, no. 22, pp. 7070–7082, 2021.
- [14] M. A. Esmail *et al.*, "On the performance of optical wireless links over random foggy channels," *IEEE Access*, vol. 5, pp. 2894–2903, 2017.
- [15] Z. Rahman *et al.*, "Performance of opportunistic receiver beam selection in multiaperture OWC systems over foggy channels," *IEEE Syst. J.*, vol. 14, no. 3, pp. 4036–4046, 2020.
- [16] A. Jurado-Navas *et al.*, "A unifying statistical model for atmospheric optical scintillation," *Numerical Simulations of Physical and Engineering Processes*, Sep 2011.
- [17] I. I. Kim *et al.*, "Comparison of laser beam propagation at 785 nm and 1550 nm in fog and haze for optical wireless communications," *Proc. SPIE*, vol. 4214, pp. 26–37, Nov. 2001.
- [18] A. A. Farid *et al.*, "Outage capacity optimization for free-space optical links with pointing errors," *J. Lightw. Technol.*, vol. 25, no. 7, pp. 1702–1710, 2007.
- [19] A. Kilbas and M. Saigo, *H-Transforms: Theory and Applications*. CRC Press., Mar. 2004.
- [20] Y. Abo Rahama *et al.*, "On the sum of independent Fox's H-function variates with applications," *IEEE Trans. Veh. Technol.*, vol. 67, no. 8, pp. 6752–6760, 2018.
- [21] I. S. Ansari *et al.*, "Performance analysis of free-space optical links over málaga (M) turbulence channels with pointing errors," *IEEE Trans. Wireless Commun.*, vol. 15, no. 1, pp. 91–102, 2016.
- [22] V. K. Chapala and S. M. Zafaruddin, "Unified performance analysis of reconfigurable intelligent surface empowered free-space optical communications," *IEEE Trans. Commun.*, pp. 1–1, *Early Access*, 2021.
- [23] Wolfram function, "https://functions.wolfram.com/hypergeometric-functions/meijerg," *Accessed Feb. 10, 2022*.
- [24] P. Mittal and K. Gupta, "An integral involving generalized function of two variables," *Proc. Indian Acad. Sci.*, vol. 75, no. 9, pp. 117–123, 1972.